Acoustic Backward-Wave Negative Refractions in the Second Band of a Sonic Crystal

Liang Feng,[1] Xiao-Ping Liu,[1] Ming-Hui Lu,[1] Yan-Bin Chen,[2] Yan-Feng Chen,[1,*] Yi-Wei Mao,[3] Jian Zi,[4] Yong-Yuan Zhu,[1] Shi-Ning Zhu,[1] and Nai-Ben Ming[1]

[1]*National Laboratory of Solid State Microstructures, Nanjing University, Nanjing 210093, China*
[2]*Department of Materials Science and Engineering, University of Michigan, Ann Arbor, Michigan 48109, USA*
[3]*Institute of Acoustics, Nanjing University, Nanjing 210093, China*
[4]*National Laboratory of Surface Physics, Fudan University, Shanghai 200433, China*

(Received 10 May 2005; published 6 January 2006)

Acoustic negative refractions with backward-wave (BW) effects were both theoretically and experimentally established in the second band of a two-dimensional (2D) triangular sonic crystal (SC). Intense Bragg scatterings result in the extreme deformation of the second band equifrequency surface (EFS) into two classes: one around the K point and the other around the Γ point of the reduced Brillouin zone. The two classes can lead to BW negative refractions (BWNRs) but with reverse negative refraction dependences on frequencies and incident angles. Not only BWNR but BW positive refraction can be present at EFSs around the K point, so it is possible to enhance the resolution of acoustic waves with a subdiffraction limit regardless of refractions, which is no analogy in both left-handed material and SCs' first band. These abundant characters make refractions in the second band distinguished.

DOI: 10.1103/PhysRevLett.96.014301 PACS numbers: 43.35.+d, 63.20.−e, 78.20.Ci

A kind of unusual material with both permittivity and permeability simultaneously negative was first predicted by Veselago in 1968, named left-handed material (LHM) because when light propagates in it, the electric field, the magnetic field, and the wave vector form a left-handed set [1]. Accompanying the left-handedness, the wave vector is opposite to the energy flow, which is called the backward-wave (BW) effect (in anisotropic media such as photonic and sonic crystals, a general situation for the BW effect should be considered as following that, although the wave vector and energy flow are always not collinear, BW still exists because the energy flow is forward but the wave vector is backward). An array of split ring resonators and wires [2–4], a kind of LHM proposed by Pendry *et al.*, has been established in experiments to realize BW negative refraction (BWNR) in microwave range by Smith *et al.* [5–7]. And through BWNRs, a superlens by LHM can be constructed to make use of both evanescent and propagating waves to produce a real subwavelength image beyond the diffraction limit due to phase compensations induced by the BW effect [8–11].

Recently, the negative refraction was also realized in photonic crystals (PCs) [12–18]. There are two cases of negative refractions in PCs. One is because of intense scatterings in the lowest band with negative refractions but without a negative index [12,13], and the other located in higher bands is the left-handed electromagnetism with a BW effect as BWNR in LHM [14–16], showing both the negative refraction and the negative refractive index. With the phase compensations by BW effects, it is also possible to obtain the transmission amplitude for evanescent waves to construct a PC based superlens [17], which was observed experimentally in the infrared region [18] and expected in the visible region.

Since last year the negative refraction has gone into acoustics, leading to an acoustic superlens based on sonic crystals (SCs) [19,20]. Although there is no corresponding left-handed set in SCs, it is still highly anticipated to obtain the acoustic BWNR with phase compensations to amplify acoustic evanescent waves. As the left-handed electromagnetism in PCs, BWNR can also exist in SCs' counterparts with an effective negative index [21,22]. Regarding the BWNR, the previous discussions [14–18,21,22] mainly defined the wave propagating along some high-symmetry directions (Γ-M or Γ-K), where the group velocity is antiparallel to the wave vector, so the refraction direction could be determined by the negative index. Except for the negative refractive index, however, in a general case with wave propagating along any directions, there are no detailed discussions about BWNR in both PC and SC, which is inevitable to stimulate us to consider more general BWNRs and find out their dependences on both frequencies and incident angles. By addressing this question in this Letter, BWNRs inside the Brillouin zone (BZ) with the wave propagating along any arbitrary low-symmetry direction are first carried out, showing more complicated and interesting characters than negative refractions in the lowest band.

In the present experiment, in order to propose a 2D triangular SC, an aluminum plate was designed to be drilled as a triangular array of holes with the lattice constant of 4.5 mm. Holes were arranged as the Γ-K direction with 99 layers in the lateral direction of the plate, and Γ-M with 20 layers in the perpendicular direction. By inserting 250-mm-long steel cylinders with the radius of 1.0 mm into the periodically drilled plate, a 2D triangular SC was constructed with steel cylinders in air background

[$\rho_{\text{steel}} = 7800\ \text{kg/m}^3$, $\rho_{\text{air}} = 1.21\ \text{kg/m}^3$, $c_{\text{steel}} = 6100\ \text{m/s}$, $c_{\text{air}} = 344.5\ \text{m/s}$ (sound velocity in air at 20 °C)].

A scanning transmission measurement of spatial distributions covering frequencies from 45.5 to 56 kHz was carried out with various incident angles. In our experiment (Fig. 1), the triangular SC with the normal as Γ-M direction was placed between two transducers (Airmar AT50, USA), one as an emitter and the other as a receiver. A 50-cycle-pulse acoustic Gaussian beam from the emitting transducer was generated by a function generator (Agilent 33120A, USA). To eliminate the angular divergence and obtain a good Gaussian shape, we used a 100-mm-long, 15-mm-thick sponge loop with an inner radius 15 mm as an absorbing waveguide between the SC and the emitting transducer. So a good Gaussian beam could be obtained by absorbing acoustic waves with large angles. The receiving transducer was mounted on a goniometer that ran along the lateral direction parallel with the SC interface (Γ-K direction). The detector was positioned at 10 cm away from the refraction surface to eliminate near field effects. In the experiment, both the emitter and the receiver were oriented to the same angle with the normal of the crystal interface. The transmission signal was acquired by a digital sampling oscilloscope with a temporal resolution of 2.5 ns. The position where the most intense signal was observed was regarded as the refraction of the acoustic wave. And the refraction was considered negative (positive) if the emerging beam is detected at the same (different) side of the surface normal as the incident beam.

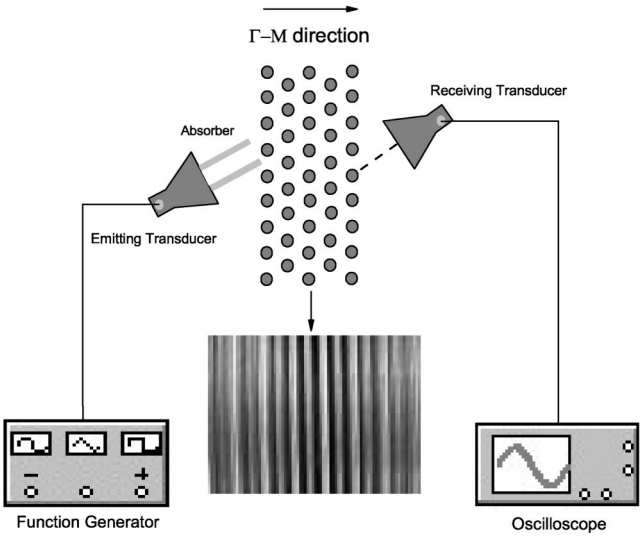

FIG. 1. Schematic of the experimental setup used to measure the transmission of ultrasonic wave in a 2D triangular SC, consisting of two transducers, an absorber, a function generator, and an oscilloscope. The SC, the rectangular slab of steel cylinders shown as the inset, is placed between two transducers with the normal as the Γ-M direction.

The BWNR in the SC could be well understood by examining the acoustic band structure and equifrequency surface (EFS). The band structure of the 2D triangular SC is calculated by both the plane wave expansions method and multiple scattering theory, which is shown in Fig. 2(a). In the second band, where the frequency of the Γ point is higher than those of other points, EFSs [Fig. 2(b)] move inwards, indicating that $v_g \cdot k < 0$. Since the group velocity is always forward (positive), the negative wave vector is expected, indicating a BW effect and producing an effective negative index $n_{\text{eff}} = k_{\text{SC}}/k_{\text{air}}$.

In studying the detailed relation of acoustic refractions, it is difficult to determine the refraction only by n_{eff} except in some particular high-symmetry directions (Γ-M or Γ-K) [14–16]. For the features inside the BZ, the propagating direction of acoustic waves must be marked in acoustic EFSs [Fig. 2(b)], in which we make a discussion on the refraction of a 30° incidence from air with the normal along the SC's Γ-M direction as we did in our experiment. With the BW effect, the right-down forward wave vector in air will find the corresponding point at the left panel of the SC's EFS because of the negative left-down wave vector in the SC, and lead to the right-up group velocity. Then in this case, the incidence and refraction stand on the same side of the interface normal (Γ-M direction), showing a BWNR.

In the second band, strong Bragg scatterings at the BZ boundaries result in the extreme deformation of EFSs of acoustic waves in the SC. The continuous EFS in the second band are dramatically distorted to several pieces, and these pieces could be presented in the reduced BZ scheme [Fig. 2(b)]. Dependent on the frequency of acoustic waves, there are different kinds of EFSs: one is the dramatically changed EFS around the K point, and the other is the gradually varying EFS around the Γ point. So there are two kinds of EFSs that lead to two different characteristic cases for BWNRs as well as their interesting relations with

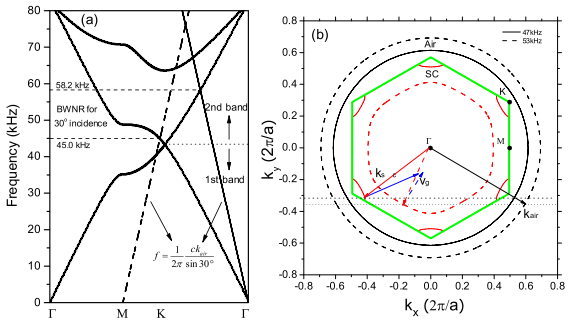

FIG. 2 (color online). Theoretical demonstrations of the acoustic negative refraction. (a) The band structure of the SC. The region between 45.0 and 58.2 kHz denotes the negative refractive frequency range for the incident beam making 30° with the SC's Γ-M direction. (b) The equifrequency surfaces in k space of the air and SC at 47.0 kHz (solid line) and 53.0 kHz (dashed line), respectively; k_{SC} and v_g are the wave vector and group velocity in the SC, respectively.

frequencies. When the frequency is below 48.8 kHz (M point), EFSs are around the K point and become larger from the K to M point. So for 30° incidence, k_{air} will find its first corresponding SC's EFS point at the K-M BZ boundary with a negative refractive angle of −90°. And when the frequency is higher, the corresponding point will be far from the BZ boundary and the EFS's curvature is less, making the refraction less negative. When the frequency is above 48.8 kHz, EFSs are around the Γ point. With the increase of frequencies, the curvature of the corresponding point at the EFS is greater, which results in a bigger negative refractive angle. And when the EFS is small enough, there exists a stopping frequency, with the negative refractive angle of −90°. To define a single beam BWNR frequency range, the similar method to determine the upper limit of all angle negative refraction could be applied here [11]. The region between two dashed lines in Fig. 2(a) denotes the BWNR frequency range from 45.0 to 58.2 kHz for 30° incidence. The dispersion line $f = \frac{1}{2\pi} \times \frac{ck_{air}}{\sin 30°}$ was calculated from both M and Γ points, whose intersections with the M-K and Γ-K directions correspond to the starting frequency 45.0 kHz and the ending frequency 58.2 kHz, respectively.

In the BWNR frequency range for 30° incidence from 45.0 to 58.2 kHz, the dependence of refractions on frequencies is shown in Fig. 3 with Fig. 3(b) the measured data represented in terms of the average transmission intensity, which agreed well with the theoretical calculation in Fig. 3(a). The negative refractive angle reached its minimum of theoretical −28.4° and experimental −32.0° at 47.0 kHz. From 45.0 to 47.0 kHz, the sharp change of the

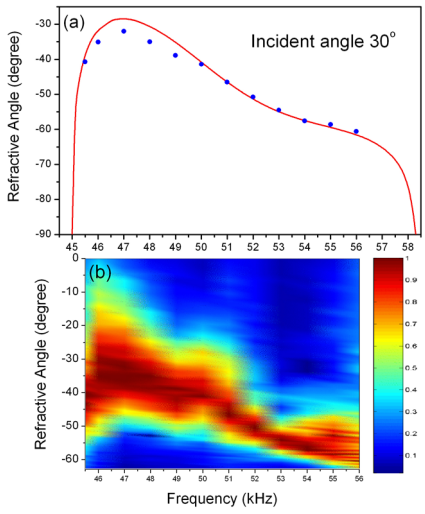

FIG. 3 (color online). The dependence of negative refractions on frequencies. (a) The comparison of experimental measurements (dots) and theoretical simulations (line) of refractive angles versus frequencies with the incident angle of 30°. (b) The average acoustic transmission intensity versus frequencies and angles with the 30° incidence. The average intensity scale varies from 0 to 1.

refraction is related to the dramatically changed EFSs around the K point due to intense Bragg scatterings. And from 47.0 to 48.8 kHz, though EFSs are still around the K point, it is the transient region for EFSs changed from the K to Γ point so that the curvature becomes greater and the refraction changes more negatively. From 48.8 to 58.2 kHz, the Bragg scatterings are less, corresponding to the gradually varying EFSs around the Γ point, and the refraction becomes more negative slowly. Hence, because of two different frequency dependent characters for EFSs, the relation of BWNRs with frequencies is not monotonically changed, different from the characters in the first band published before [12,18,19].

BWNRs are also strongly dependent on the incident angles of the acoustic beam. For both different BWNRs, however, the dependences of refractions on incident angles are reverse. The SC's EFSs (Fig. 2) could also be used to describe relations between negative refractions and incident angles at a constant frequency. For the EFS around the K point at 47.0 kHz, there are two directional band gaps, one as the incident angle from 0° to 21.4° and the other from 38.6° to 90°. Only when the incident angle is between 21.4° and 38.6° can k_{air} find its corresponding SC's EFS point, which also first takes place at the K-M BZ boundary, producing the negative refractive angle of −90° with the incident angle of 21.4°. And with raising the incident angles, the refraction will become from negative to positive, and reach its positive maximum 30° with the incident angle of 38.6°. While for the EFS around the Γ point at 53.0 kHz, the EFS is smaller than air's so that the acoustic wave will experience total internal reflection and no refraction exists if the angle of incidences is greater than 43.6°. With enlarging the incident angle from 0° to 43.6°, the refractive angle will monotonically change to be more negative from 0° to −90°. To demonstrate this effect, the angles of refractions are theoretically calculated and experimentally measured with a variety of incident angles at 47.0 and 53.0 kHz as depicted in Fig. 4, showing good agreements between theoretical calculations and experiment measurements. So both absolutely reverse refractions might result in the abundant nature of refractions in arbitrary directions and lead to some additional interesting effects, such as BW positive refraction (BWPR).

BW effects taking place in the second band of SCs are quite different from that in LHM and SC's first band as shown in the illustration Fig. 5. In fact, BWNR inherent from EFSs around the Γ point in the second band is something like the negative refractions in LHM [2–7] where an effective negative index results in approximately isotropic EFSs. However, EFSs around the K point attribute to two kinds of BW effects including both BWNR and BWPR. Especially for the BWPR, there is no analogy in both LHM and SC's first band. These abundant characters are attributed to the extremely distorted EFSs due to intense Bragg scatterings near BZ boundaries. Hence in the second band,

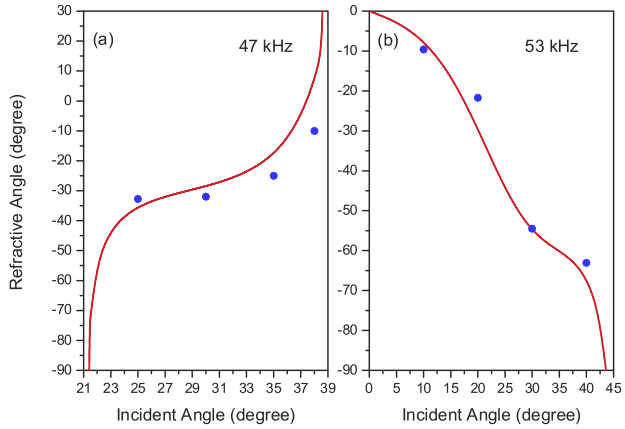

FIG. 4 (color online). Comparisons of measured (dots) and calculated (line) angles of refractions versus angles of incidences at 47.0 (a) and 53.0 kHz (b).

BWPR is the most important character distinguished from both LHM and the first band. Comparing to these effects in PC's second band, BWNR and BWPR in SC are analogous to left-handed negative and positive refractions in PC, respectively. With BW effect induced phase compensations, regardless of BWNR and BWPR, evanescent waves in the second band are always amplified to enhance the resolution of acoustic waves with a subdiffraction limit [11].

To summarize, the acoustic negative refraction with BW effects in the second band of a 2D triangular SC was experimentally established and theoretically analyzed inside the BZ. Resulted from the intense scatterings near the BZ boundary, two different EFSs around K and Γ points, respectively, in the second band attribute to two kinds of absolutely reverse BWNRs as well as their interesting dependences on both frequencies and incident angles. In the second band, both BWNR and BWPR exist, which is distinguished from that in the SC's first band and LHM. With phase compensations, BW effects in our SC provide the possibilities to obtain the transmission amplitude for evanescent waves with both negative and positive refractions, then enhance the resolution of acoustic waves and obtain an acoustic subwavelength image, which have great potential in ultrasonic biosensing and medical measurements. And this effect could also extend to PC and other wave propagations in the periodic structures, exhibiting a universal promise.

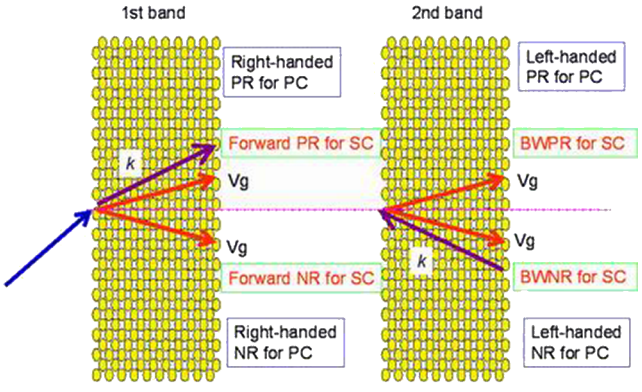

FIG. 5 (color online). Illustration of refractions in both the first and second bands of SC, as well as their counterparts in PC.

The work was jointly supported by the National 863 High Technology Program, the State Key Program for Basic Research of China, and the National Nature Science Foundation of China (Grant No. 50225204).

*Electronic address: yfchen@nju.edu.cn

[1] V. G. Veselago, Sov. Phys. Usp. **10**, 509 (1968).
[2] J. B. Pendry, A. J. Holedn, W. J. Stewart, and I. Youngs, Phys. Rev. Lett. **76**, 4773 (1996).
[3] J. B. Pendry, A. J. Holedn, D. J. Robbins, and W. J. Stewart, J. Phys. Condens. Matter **10**, 4785 (1998).
[4] J. B. Pendry, A. J. Holedn, D. J. Robbins, and W. J. Stewart, IEEE Trans. Microw. Theory Tech. **47**, 2075 (1999).
[5] D. R. Smith, W. J. Padilla, D. C. Vier, S. C. Nemat-Nasser, and S. Schultz, Phys. Rev. Lett. **84**, 4184 (2000).
[6] R. A. Shelby, D. R. Smith, S. C. Nemat-Nasser, and S. Schultz, Appl. Phys. Lett. **78**, 489 (2001).
[7] R. A. Shelby, D. R. Smith, and S. Schultz, Science **292**, 77 (2001).
[8] J. B. Pendry, Phys. Rev. Lett. **85**, 3966 (2000).
[9] A. A. Houck, J. B. Brock, and I. L. Chuang, Phys. Rev. Lett. **90**, 137401 (2003).
[10] L. Feng, X. P. Liu, M. H. Lu, and Y. F. Chen, Phys. Lett. A **332**, 449 (2004).
[11] N. Fang, H. Lee, C. Sun, and X. Zhang, Science **308**, 534 (2005).
[12] C. Luo, S. G. Johnson, J. D. Joannopoulos, and J. B. Pendry, Phys. Rev. B **65**, 201104(R) (2002).
[13] E. Cubukcu, K. Aydin, E. Ozbay, S. Foteinopoulou, and C. M. Soukoulis, Nature (London) **423**, 604 (2003).
[14] M. Notomi, Phys. Rev. B **62**, 10 696 (2000).
[15] S. Foteinopoulou and C. M. Soukoulis, Phys. Rev. B **67**, 235107 (2003).
[16] P. V. Parimi, W. T. Lu, P. Vodo, J. Sokoloff, J. S. Derov, and S. Sridhar, Phys. Rev. Lett. **92**, 127401 (2004).
[17] K. Guven, K. Aydin, K. B. Alici, C. M. Soukoulis, and E. Ozbay, Phys. Rev. B **70**, 205125 (2004).
[18] A. Berrier, M. Mulot, M. Swillo, M. Qiu, L. Thylén, A. Talneau, and S. Anand, Phys. Rev. Lett. **93**, 073902 (2004).
[19] X. Zhang and Z. Liu, Appl. Phys. Lett. **85**, 341 (2004).
[20] S. Yang, J. H. Page, Z. Liu, M. L. Cowan, C. T. Chan, and P. Sheng, Phys. Rev. Lett. **93**, 024301 (2004).
[21] J. H. Page, A. Sukhovich, S. Yang, M. L. Cowan, F. Van Der Biest, A. Tourin, M. Fing, Z. Liu, C. T. Chan, and P. Sheng, Phys. Status Solidi B **241**, 3454 (2004).
[22] C. Qiu, X. Zhang, and Z. Liu, Phys. Rev. B **71**, 054302 (2005).